

Magnetotellurics with a remote magnetic reference

T. D. Gamble,* W. M. Goubau,* and J. Clarke*

Magnetotelluric measurements were performed simultaneously at two sites 4.8 km apart near Hollister, California. SQUID magnetometers were used to measure fluctuations in two orthogonal horizontal components of the magnetic field. The data obtained at each site were analyzed using the magnetic fields at the other site as a remote reference. In this technique, one multiplies the equations relating the Fourier components of the electric and magnetic fields by a component of magnetic field from the remote reference. By averaging the various crossproducts, estimates of the impedance tensor not biased by noise are obtained, provided there are no correlations between the noises in the remote channels and noises in the local channels. For some data, conventional methods of analysis yielded estimates of apparent resistivities that were biased by noise by as much as two orders of magnitude. Nevertheless, estimates of the apparent resistivity obtained from these same data, using the remote reference technique, were consistent with apparent resistivities calculated from relatively noise-free data at adjacent periods. The estimated standard deviation for periods shorter than 3 sec was less than 5 percent, and for 87 percent of the data, was less than 2 percent. Where data bands overlapped between periods of 0.33 sec and 1 sec, the average discrepancy between the apparent resistivities was 1.8 percent.

INTRODUCTION

In the magnetotelluric (MT) method, one seeks the elements of the impedance tensor $Z(\omega)$ from the equations

$$E_x(\omega) = Z_{xx}(\omega)H_x(\omega) + Z_{xy}(\omega)H_y(\omega), \quad (1)$$

and

$$E_y(\omega) = Z_{yx}(\omega)H_x(\omega) + Z_{yy}(\omega)H_y(\omega). \quad (2)$$

In equations (1) and (2), $H_x(\omega)$, $H_y(\omega)$, $E_x(\omega)$, and $E_y(\omega)$ are the Fourier transforms of the fluctuating horizontal magnetic (H) and electric (E) fields $H_x(t)$, $H_y(t)$, $E_x(t)$, and $E_y(t)$. If one multiplies equations (1) and (2) in turn by the complex conjugate of each of the frequency-dependent fields, and averages the resulting autopowers and crosspowers of the fields over many sets of data, one obtains eight simultaneous equations that can be solved for the impedance elements. As is well known, the autopowers may severely bias the impedance estimates if there is noise in the measured fields (Sims et al, 1971; Kao and Rankin, 1977). An earlier

paper (Goubau et al, 1978) discussed two different approaches to reducing this bias, namely, (1) a solution of the eight simultaneous equations for the impedance elements in terms of crosspowers alone, and (2) a solution of the equations in terms of weighted crosspowers. Analysis techniques for MT measurements with a fifth (electric or magnetic) local reference channel were also discussed, including a crosspower analysis in which one multiplies equations (1) and (2) by the complex conjugate of the Fourier transform of the reference field. It was concluded that any of the 4- or 5-channel methods would work satisfactorily provided that the noise in the various channels was uncorrelated. These techniques were tested on data obtained at Grass Valley, Nevada. In most measurements, there was a significant level of correlated noise found between some channels. Most techniques yielded apparent resistivities that were biased.

Finally, use of a remote magnetometer was proposed to obtain reference fields $H_{xr}(t)$ and $H_{yr}(t)$ in which the noise should be uncorrelated with any of the

Manuscript received by the Editor February 10, 1978; revised manuscript received April 17, 1978.

*University of California, Materials and Molecular Research and Earth Sciences Division, Lawrence Berkeley Laboratory, Berkeley, CA 94720.

0016-8033/79/0101-0053\$03.00. © 1979 Society of Exploration Geophysicists. All rights reserved.

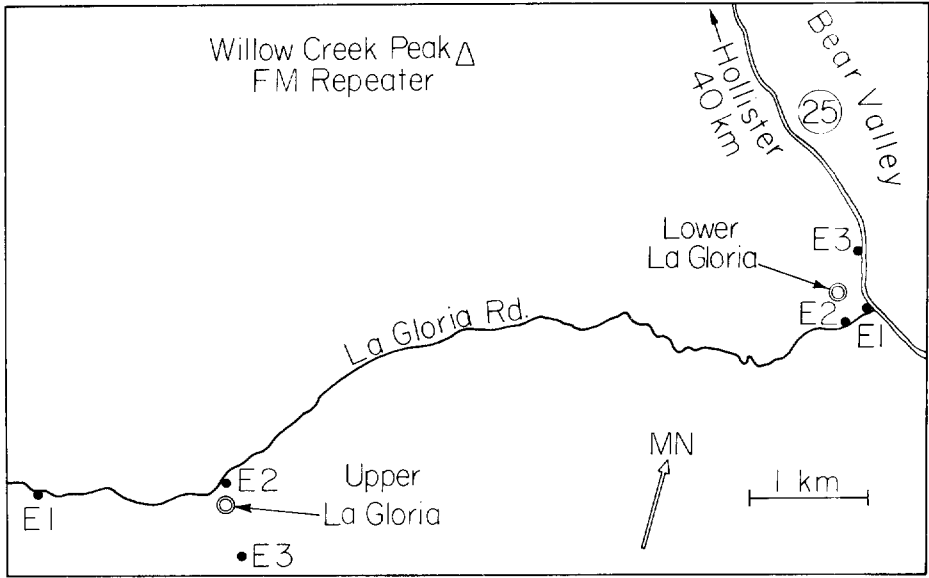


FIG. 1. Magnetotelluric measurement sites in Bear Valley, California, \odot magnetometer; \bullet electrode.

four fields at the MT station. Equations (1) and (2) can be solved by multiplying them in turn by $H_{xr}^*(\omega)$ and $H_{yr}^*(\omega)$ to obtain four more equations that can be solved for the impedance elements. One finds:

$$Z_{xx} = (\overline{E_x H_{xr}^* H_y H_{yr}^*} - \overline{E_x H_{yr}^* H_y H_{xr}^*}) / D, \quad (3)$$

$$Z_{xy} = (\overline{E_x H_{yr}^* H_x H_{xr}^*} - \overline{E_x H_{xr}^* H_x H_{yr}^*}) / D, \quad (4)$$

$$Z_{yx} = (\overline{E_y H_{xr}^* H_y H_{yr}^*} - \overline{E_y H_{yr}^* H_y H_{xr}^*}) / D, \quad (5)$$

and

$$Z_{yy} = (\overline{E_y H_{yr}^* H_x H_{xr}^*} - \overline{E_y H_{xr}^* H_x H_{yr}^*}) / D, \quad (6)$$

where

$$D \equiv \overline{H_x H_{xr}^* H_y H_{yr}^*} - \overline{H_x H_{yr}^* H_y H_{xr}^*}.$$

The bar denotes an average over all transform points within a given frequency window, and over all sets of data. The impedance elements will be unbiased by noise provided the noise in the MT array is uncorrelated with noise in the reference channels. It should be noted that since equation (1) and then (2) is multiplied in turn by a single reference field, the values of the impedance elements are independent of the magnitudes and phases of the reference fields. Therefore, one does not need a precise knowledge of the gains or phase shifts in the telemetry for the remote references.

In this paper, a test of the remote reference technique is described. In Bear Valley, near Hollister, California, two magnetotelluric stations were set up

and E_x , E_y , H_x , H_y , and H_z were recorded from both stations simultaneously. The standard analysis techniques yielded apparent resistivities that were significantly biased by noise. However, the use of the remote reference allowed derivation of apparent resistivities that had no obvious bias, even when the coherencies were as low as 0.1. Furthermore, where the highest frequency band and second highest frequency band overlapped, the apparent resistivities agreed to within 1.8 percent. The estimated standard deviation for the apparent resistivities at periods shorter than 3 sec was 1.3 percent.

MEASUREMENTS

Two complete MT stations separated by 4.8 km were established on La Gloria road in Bear Valley, California, at the sites shown in Figure 1. The Upper La Gloria station is in hilly terrain where the geology consists chiefly of granites, while the Lower La Gloria station is in a level area over a zone of low resistivity (Mazella, 1976), and is slightly east of a fault that separates this zone from the granites. Lower La Gloria is about 2 km west of the San Andreas rift zone.

The Pb electrodes installed by Corwin for dipole-dipole resistivity monitoring were used for the electric field measurements (Morrison et al, 1977). The location of the electrodes is shown in Figure 1. Electrodes E_1 and E_2 were the common electrodes at the lower and upper stations, respectively. In the subsequent

analysis, the electric field directions at each station were made orthogonal. For the magnetic field measurements a dc SQUID 3-axis magnetometer (Clarke et al, 1976) at Lower La Gloria, and an rf SQUID 3-axis magnetometer, manufactured by S.H.E. Corporation, at Upper La Gloria were used. The magnetic field sensitivities were approximately $10^{-5} \gamma \text{Hz}^{-1/2}$ and $10^{-4} \gamma \text{Hz}^{-1/2}$, respectively. The magnetometer at each site was used as the reference for the MT signals at the other site.

The MT data and the vertical components of the magnetic field fluctuations at each site were recorded simultaneously. A block diagram of the measurement electronics appears in Figure 2. The equipment at Lower La Gloria was battery powered, while that at Upper La Gloria was powered by a 60 Hz generator. Each signal was passed through a preamplifier that contained a high-pass filter to attenuate the large-amplitude low-frequency signals that could have exceeded the dynamic range of the electronic circuits. Each preamplifier was followed by a 60 Hz notch filter. The signals from Lower La Gloria were transmitted to Upper La Gloria via FM telemetry via a repeater on Willow Creek Peak. At Upper La Gloria we passed each of the eight MT signals and two vertical components of magnetic field through a four-pole band-pass filter, digitized the signals with 12-bit resolution, and recorded the data on a nine-track digital recorder. Data were acquired in the four overlapping bands listed in Table 1. Band 4 was intended to include periods from 30 to 1000 sec, but an error in setting the high-pass filter of the telemetry preamplifier at the remote site resulted in the longest period being 100 sec. The times required for data collection

Table 1. Summary of filter bands, total recording time per band, digitizer sampling period, and the number of points per fast Fourier transform (FFT).

Filter band no.	Filter band (sec)	Total recording time (hours)	Digitizer sampling periods (sec)	No. of points per FFT
1	0.02-1	0.54	0.005	1024
2	0.33-5	4.22	0.1	512
3	3-100	10.52	1	512
4	30-100	14.9	10	256

and the sampling periods are also listed in Table 1. All data were recorded within a 40 hour period, with only brief interruptions to change gains, filter bands, and batteries.

DATA PROCESSING

The CDC 7600 computer facility of the Lawrence Berkeley Laboratory, data was used for data processing, graphed on microfilm, and the records visually inspected. After data rendered meaningless by equipment failure, amplifier saturation, or magnetic interference from passing vehicles were rejected, the remaining data were arranged into segments containing the number of points shown in Table 1. The mean value and linear trend was subtracted from each segment. The ends of the segments were multiplied by a cosine bell window, and the fast Fourier transform was computed. The necessary crosspower and autopower densities were calculated by multiplying the Fourier coefficients for the various fields together, and averaging the products over all

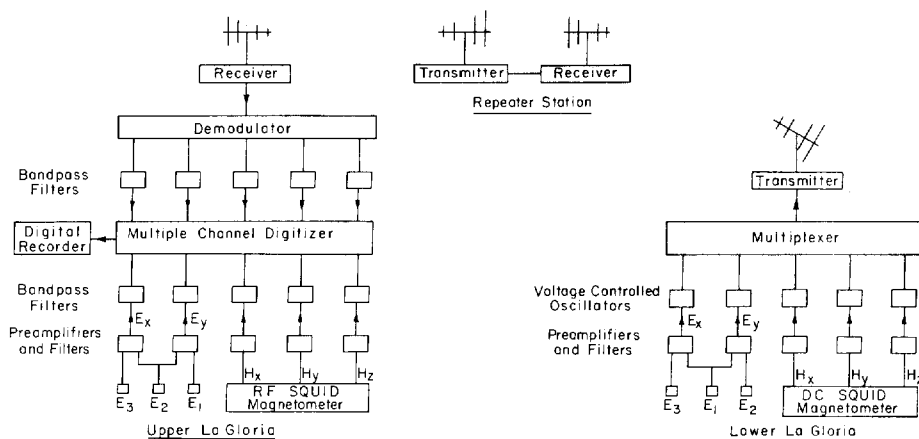


FIG. 2. Block diagram of data acquisition.

Table 2. Number of harmonics per window, and numbers of sets of data segments for each station.

Band no. 1		Band no. 2		Band no. 3		Band no. 4	
Period (sec)	Harmonics per window	Period (sec)	Harmonics per window	Period (sec)	Harmonics per window	Period (sec)	Harmonics per window
0.023	75	0.325	52	3.3	52	32.0	13
0.032	53	0.45	37	4.5	37	41.1	9
0.044	38	0.63	27	6.3	27	60.9	7
0.062	27	0.88	19	8.8	19	85.3	5
0.085	19	1.2	14	12	14		
0.12	14	1.7	10	17	10		
0.16	10	2.4	7	24	7		
0.22	7	3.4	5	34	5		
0.30	5			49	4		
0.41	4						
0.57	3						
0.79	2						

Number of sets of data segments			
Upper La Gloria			
476	297	74	21
Lower La Gloria			
381	297	74	21

of the data segments and over the Fourier harmonics contained in nonoverlapping frequency windows of $Q = 3$. The center period of each window, the number of harmonics in each window, and the number of segments are given in Table 2.

DATA ANALYSIS

Impedance tensors were computed for both MT stations as a function of period using equations (3) to (6). For comparison the impedance tensors were also computed using the following three methods: (1) The impedance tensor was found that minimized the mean square of $|\mathbf{E} - \mathbf{ZH}|$. This method is referred to as the standard analysis since it is the method that is most commonly used (Vozoff, 1972). Impedances calculated by this method depend on autopowers of the magnetic fields. As a result, magnitudes of the impedance tensor elements are biased downward by the noise power in the magnetic channels. (2) Z was computed from the inverse of the admittance tensor Y , where Y was chosen to minimize the mean square of $|\mathbf{H} - \mathbf{YE}|$. This calculation is referred to as the admittance method which biases the magnitudes of the impedance tensor elements upward by the noise power in the electric fields (Sims et al, 1971). (3) Z was computed in terms of crosspowers of the four fields measured at each station. As we have shown (Goubau et al, 1978), there is sufficient information in the crosspower data to enable one to obtain estimates of Z that are not biased by the noise power in any of the channels. We refer to this analysis as the crosspower method.

For each method of analysis the coordinate axes were rotated to maximize $|Z_{xy}|^2 + |Z_{yx}|^2$, thereby aligning one of the axes parallel to the strike direction, if such a direction existed. Then the off-diagonal elements, ρ_{xy} and ρ_{yx} , of the rotated apparent resistivity matrix were computed from the expressions

$$\rho_{xy} = 0.2 |Z_{xy}|^2 T, \quad (7)$$

and

$$\rho_{yx} = 0.2 |Z_{yx}|^2 T, \quad (8)$$

where ρ_{xy} and ρ_{yx} are in Ωm , T is the period in seconds, and Z_{xy} and Z_{yx} are in units of $(\text{mV}/\text{km}) \gamma^{-1}$. For the standard and remote reference analyses, the phases of Z_{xy} and Z_{yx} and the skewnesses $|(Z_{xx} + Z_{yy}) / (Z_{yx} - Z_{xy})|$ also were calculated.

To obtain an estimate of the noise in our data, we computed the coherency between the measured electric field \mathbf{E} and the electric field \mathbf{E}_p predicted from $\mathbf{E}_p = \mathbf{ZH}$, where Z was obtained from the standard analysis. The coherencies are defined by $C_i = \overline{E_i E_{ip}^*} / (\overline{|E_i|^2} \overline{|E_{ip}|^2})^{1/2}$, where $i = x, y$. For the standard analysis one can show that $\overline{E_i E_{ip}^*} = \overline{|E_{ip}|^2}$, so that

$$C_i = (\overline{|E_{ip}|^2} / \overline{|E_i|^2})^{1/2} \quad (i = x, y). \quad (9)$$

GRAPHICAL COMPARISON OF APPARENT RESISTIVITIES

The results for Upper La Gloria are summarized in Figures 3 to 9, and for Lower La Gloria in Figures 10 to 16. Figures 3 through 6 show the apparent resistivities as a function of period for the standard, admit-

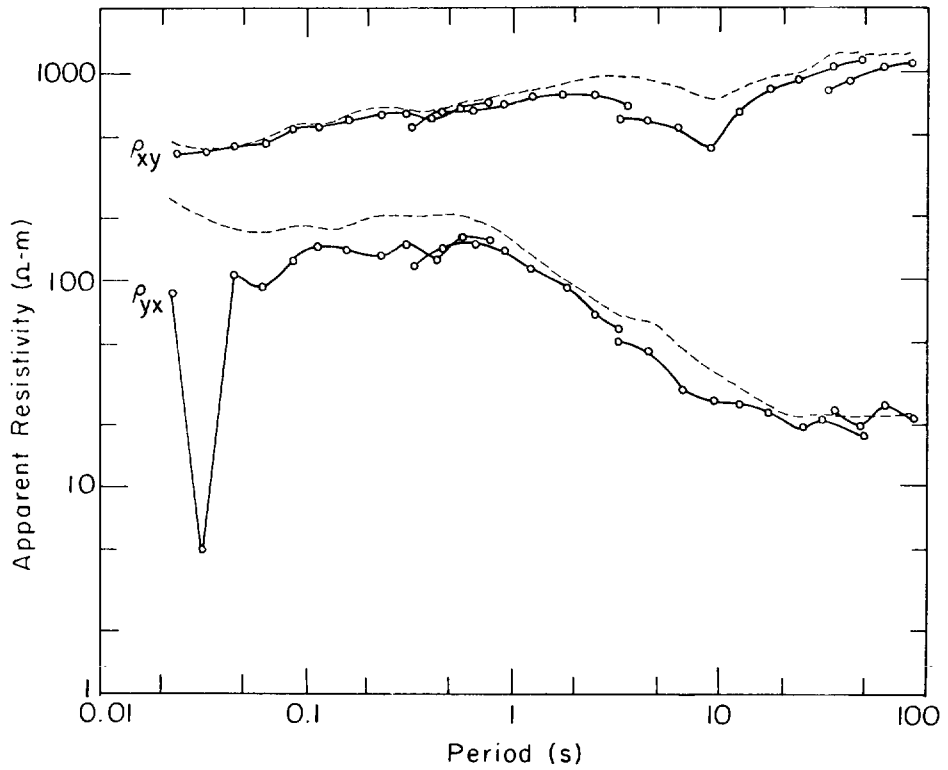


FIG. 3. Standard method apparent resistivities versus period, Upper La Gloria. Remote reference results are indicated by dashed lines.

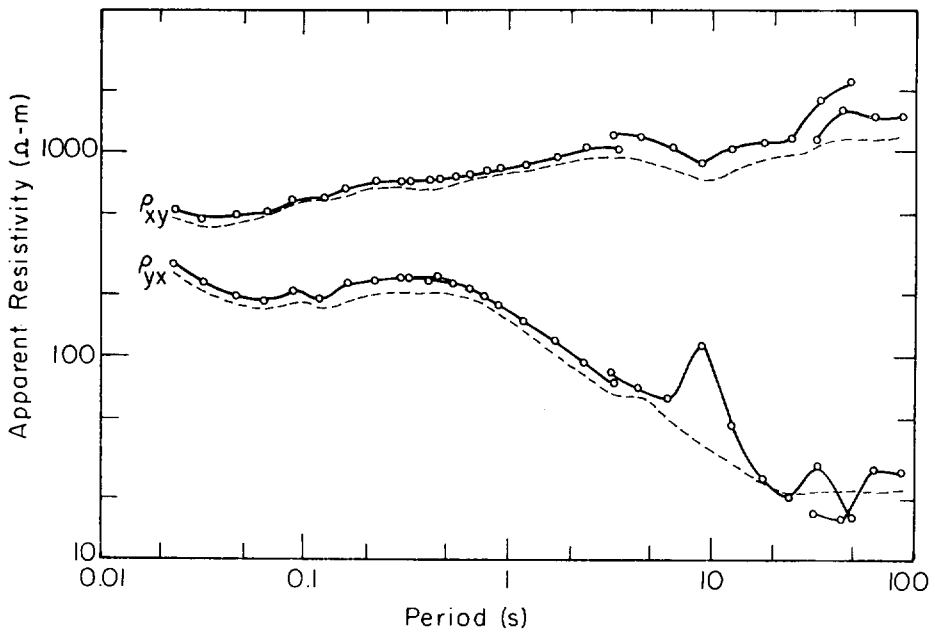


FIG. 4. Admittance method apparent resistivities versus period, Upper La Gloria. Remote reference results are indicated by dashed lines.

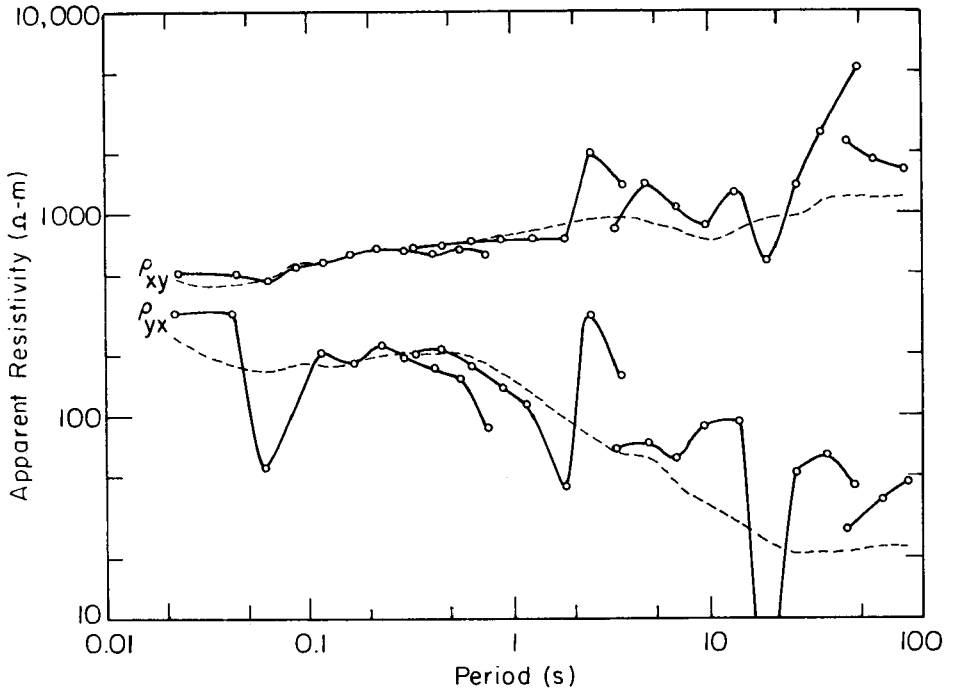


FIG. 5. Crosspower method apparent resistivities versus period, Upper La Gloria. Remote reference results are indicated by dashed lines.

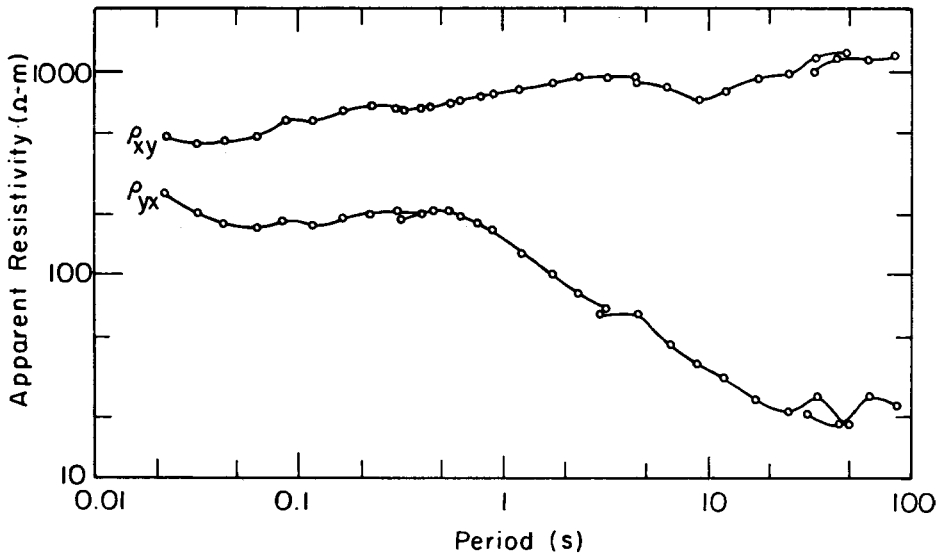


FIG. 6. Remote reference method apparent resistivities versus period, Upper La Gloria.

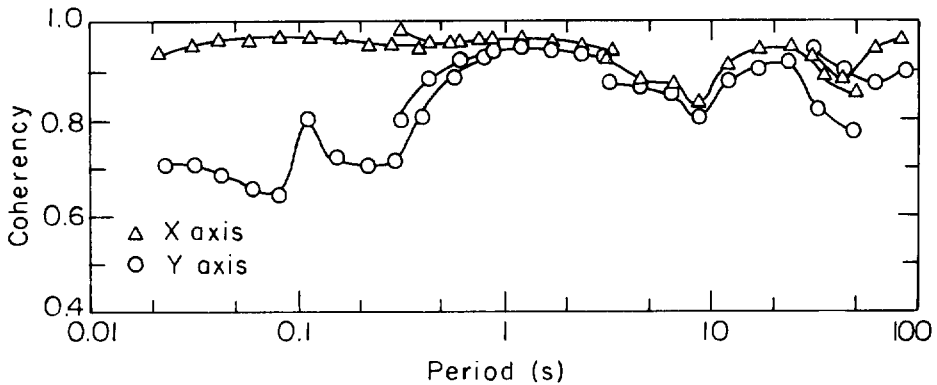


FIG. 7. Coherency between the measured electric field and the electric field predicted by the standard method of analysis, Upper La Gloria.

tance, crosspower, and remote reference methods at the Upper La Gloria station.¹ The apparent resistivities from the remote reference method are repeated as dashed lines on Figures 3 to 5 to facilitate comparison with the other methods. The coherencies C_x and C_y are plotted in Figure 7.

Comparing Figures 3 and 4, we see that both the standard and admittance methods yield resistivities that vary smoothly over wide ranges of periods. However, both methods yield discontinuities in ρ_{xy} where bands overlap at periods of 3 and 30 sec. These discontinuities will be discussed later, and it will be shown that they are not caused by systematic errors in data processing. The standard analysis also shows a large dip in ρ_{yx} at 0.03 sec that does not appear in the admittance results, and is not associated with any anomaly in C_y (Figure 7). This dip is believed to be caused by the magnetic noise from the generator at the Upper La Gloria station.

Although the apparent resistivity curves from the standard and admittance methods are fairly smooth, there are significant systematic discrepancies. The resistivities from the admittance analysis are higher than those from the standard analysis in all cases except four on the y -axis near 40 sec period. By comparing Figures 3 and 4 with Figure 7 one sees that the discrepancies generally increase as the coherency C_i decreases. The best agreement between the two methods is for periods shorter than 2 sec. For periods

shorter than 3 sec, C_x is greater than 0.9, and most values of ρ_{xy} in Figure 4 are about 10 percent higher than those in Figure 3, although the disagreement does increase to a factor of 2 at 3 sec period. For C between 0.9 and 0.6, the disagreement is usually about a factor of two (for example, ρ_{yx} between 0.06 and 1 sec periods), but can be much larger (for example ρ_{yx} at 0.032 and 9 sec periods). The systematic differences are attributed to the bias errors mentioned earlier.

The apparent resistivities from the crosspower method (Figure 5) are far more irregular than those from the admittance (Figure 4) or standard (Figure 3) methods. The random errors of the crosspower analysis depend in a complex way on the value of the impedance tensor, the orientation of the measurement axes, and the relative levels of the noises. However, we believe that the random errors are relatively large primarily because this estimate of the impedance tensor depends strongly on the crosspowers between fields that may be only slightly coherent, such as $\overline{E_x E_y^*}$ (Goubau et al, 1978). The best results from this method are for ρ_{xy} at periods shorter than 1 sec, where C_x is greater than 0.9. Here, the resistivities from the crosspower method are still scattered over the 10 percent range of the disagreement between the standard and admittance resistivities. Note that no value of apparent resistivity has been plotted at 0.032 sec period for the crosspower method (Figure 5). This is because this method did not predict real values for the auto-powers. Thus, there is some significant noise in this window even though C_y is higher than in the adjacent windows (Figure 7).

Because of the large random errors in the crosspower analysis and the bias errors in the two least-squares analyses, these methods cannot be used to

¹The windows at 0.023 sec and 0.325 sec contain harmonics outside the band-pass of the filters, and ordinarily would not be used. However, we plotted the apparent resistivities from the 0.023 sec window to demonstrate the narrow band nature of the noise in the 0.032 sec window. The apparent resistivities from the 0.325 sec window were used only to interpolate a value of the resistivity to be compared with the result at 0.41 sec from band 1.

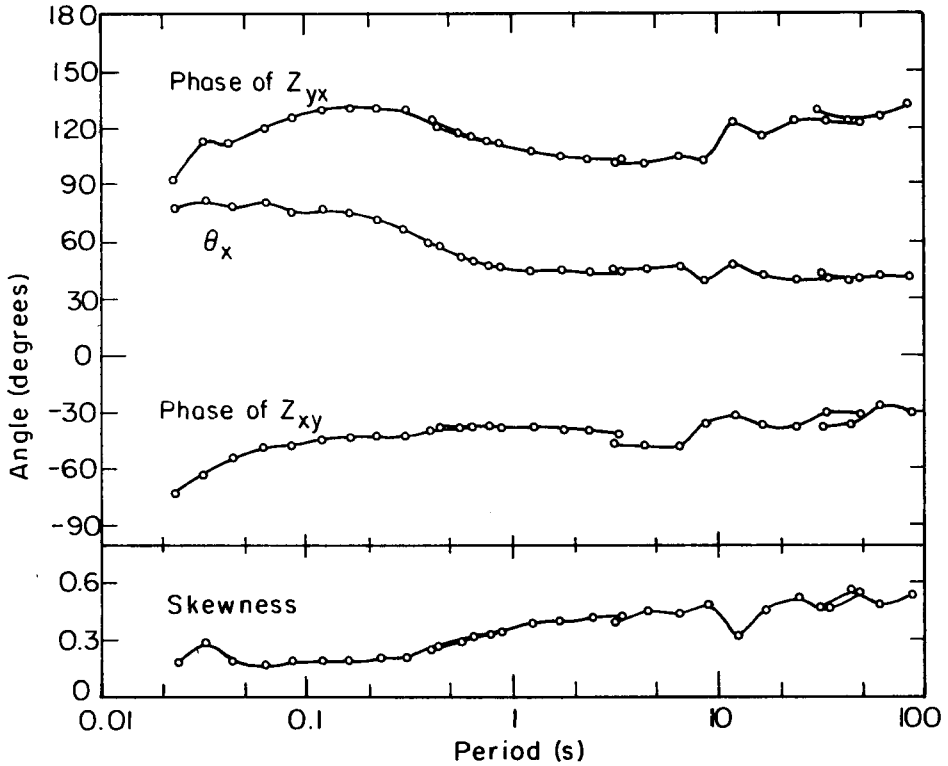


FIG. 8. Orientation angle θ_x between rotated x -axis and magnetic north, skewness, and phase angles versus period, standard method, Upper La Gloria.

obtain reliable estimates of the apparent resistivity when the C_i are less than 0.9. If all resistivities for which C_i is below 0.9 sec were rejected, only 11 values for ρ_{yx} would be retained, all at periods longer than 0.5 sec.

In Figure 6 the apparent resistivities from the remote reference method lie on smoother curves than those from any of the previous methods. Furthermore, the discontinuities and disagreements where bands overlap in Figures 3 and 4 have essentially been eliminated, suggesting that the disagreements were caused by bias errors. In the next section, we compare quantitatively the results from different bands where the bands overlap. At periods where the C_i are high, the remote reference usually agrees well with the standard and admittance methods. For ρ_{xy} between 0.032 and 2 sec, the apparent resistivities obtained using the remote reference lie about half-way between, and are within about 5 percent of those obtained with the standard and admittance methods.

We produced 64 apparent resistivities from each method of analysis at Upper La Gloria. In 60 cases the apparent resistivities from the admittance method are

larger, and those from the standard method are smaller than those from the remote reference method. This regular ordering of the apparent resistivities demonstrates that the bias error in at least two of the methods is large compared to the random error in any of them and it strongly suggests that the bias is due to the use of autopower estimates in the least-squares methods.

The apparent resistivities at Lower La Gloria from the standard, admittance, crosspower, and remote reference methods are shown in Figures 10 to 13, and the electric field predicted coherencies C_x and C_y are shown in Figure 14. Again, the dashed lines in Figures 10 to 12 reproduce the remote reference apparent resistivities from Figure 13. At Lower La Gloria there was more noise than at the upper station. C_x and C_y are never both above 0.9. C_x and C_y are both below 0.5 for periods between 5 and 10 sec. At all periods, the apparent resistivities from the admittance method (Figure 11) are higher than the corresponding apparent resistivities from the standard analysis (Figure 10). Thus, as at Upper La Gloria, the bias errors of the least-squares methods are large compared to the random errors. When C_i is lowest, the

relative bias is largest. At a period of 9 sec the relative bias is about a factor of 20 for ρ_{yx} , and about a factor of 100 for ρ_{xy} . The peaks and dips in the apparent resistivity curves in Figures 10 and 11 are also so steep that neither least-squares method accurately estimates the apparent resistivity of the ground.

The apparent resistivities from the crosspower analysis at Lower La Gloria (Figure 12) seem to be more stable than they were at Upper La Gloria (Figure 5). For periods shorter than 20 sec the crosspower method yields apparent resistivities that lie between the two least-squares resistivities in 50 of 54 cases. This result indicates that the random errors for the crosspower method are small in this case compared to the bias errors of the least-squares methods, and is further evidence that the autopower bias is the major source of error. At periods between 3 and 20 sec, the crosspower analysis yields dips in the apparent resistivity similar to those of the standard analysis, but about a factor of five smaller. Such dips are believed to be caused by correlations in the noises, which bias the estimates of the apparent resistivity.

Table 3. Percent disagreement in apparent resistivities between bands.

Bands	Remote reference	Standard	No. of values compared
1, 2	1.8	5.9	12
2, 3	4.5	41.5	4
3, 4	6.3	11.5	8

In contrast with the other methods, the remote reference method yields apparent resistivities (Figure 13) that vary smoothly over the entire range of periods, even where the coherency is low. There is almost no disagreement between overlapping bands. At periods shorter than 1 sec, the remote reference apparent resistivities agree with the results from the crosspower method to within the random scatter of the crosspower results (± 10 percent). The resistivities from the standard method are biased downward by about 10 percent near 1 sec period, and by more than a factor of 2 at the shortest periods.

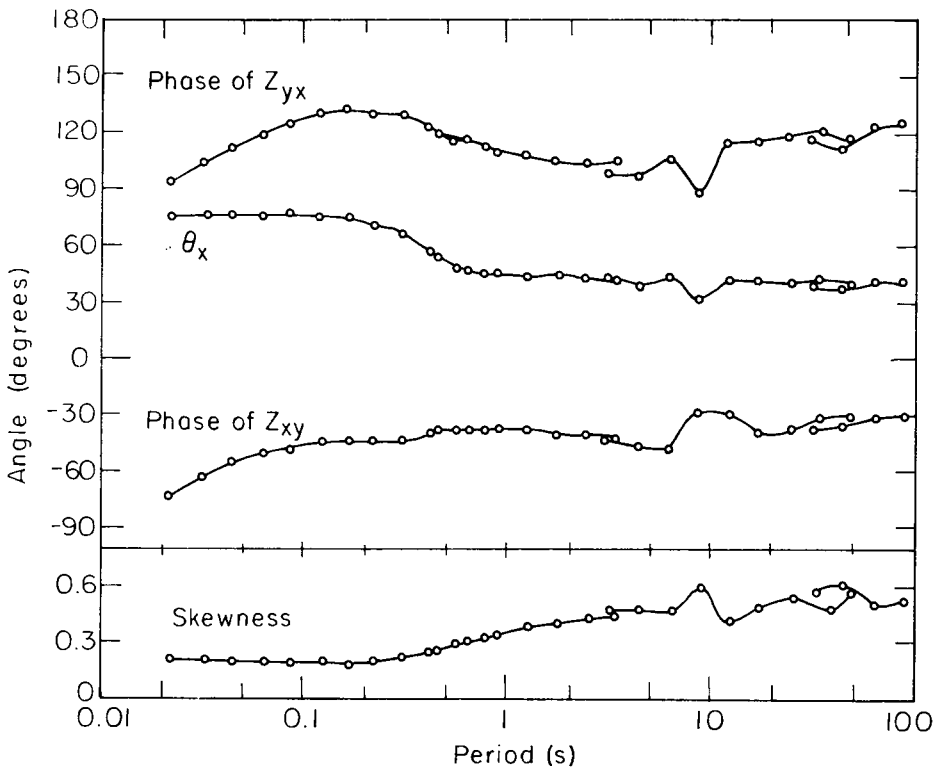


FIG. 9. Orientation angle θ_x between rotated x -axis and magnetic north, skewness, and phase angles versus period, remote reference method, Upper La Gloria.

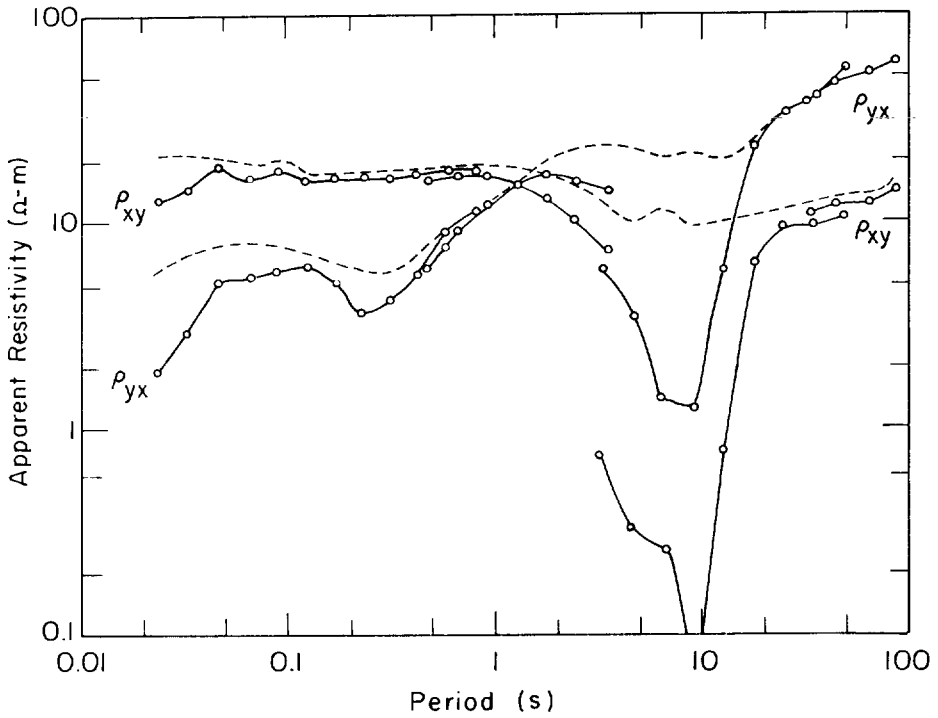


FIG. 10. Standard method apparent resistivities versus period, Lower La Gloria. Remote reference results are indicated by dashed lines.

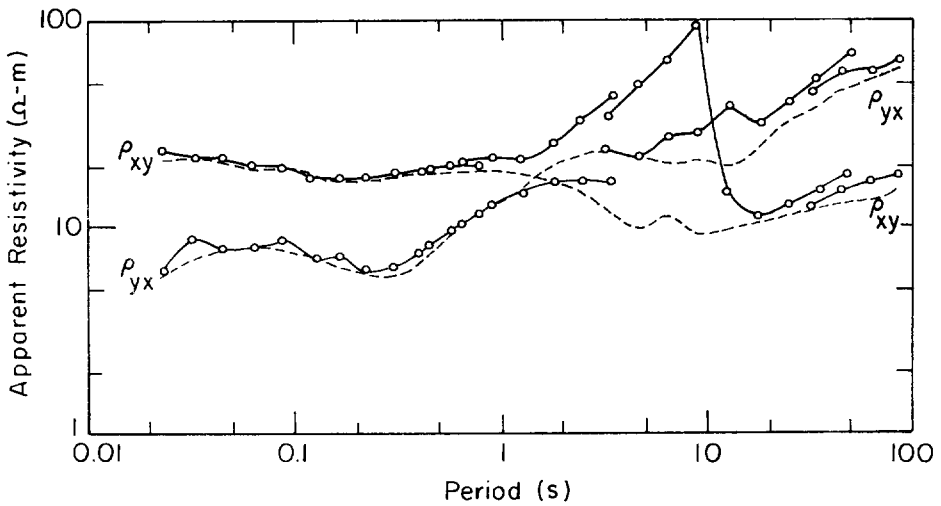


FIG. 11. Admittance method apparent resistivities versus period, Lower La Gloria. Remote reference results are indicated by dashed lines.

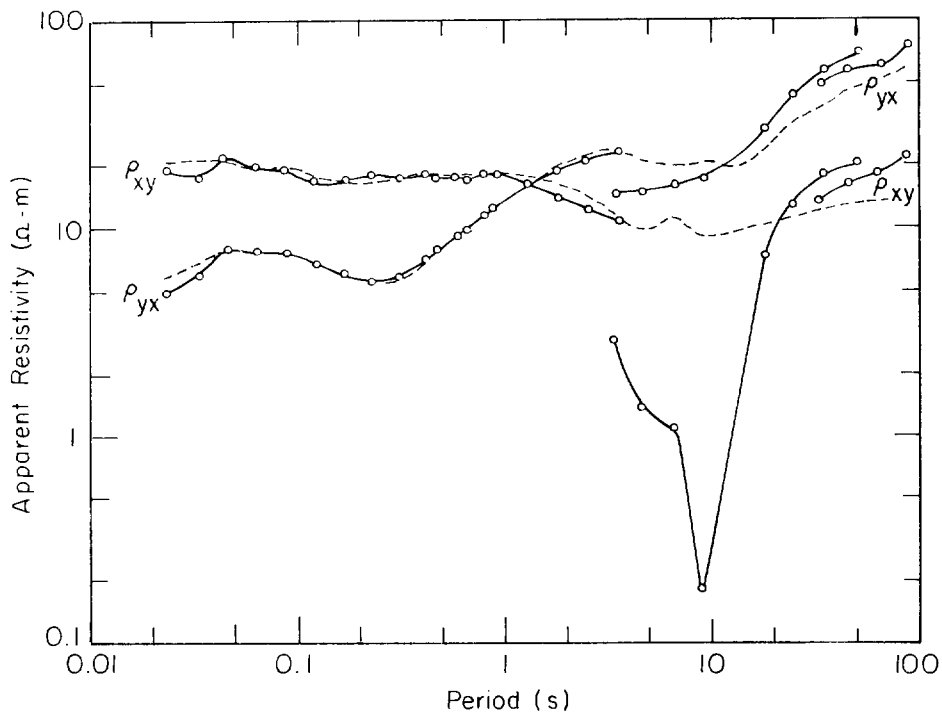


FIG. 12. Crosspower method apparent resistivities versus period, Lower La Gloria. Remote reference results are indicated by dashed lines.

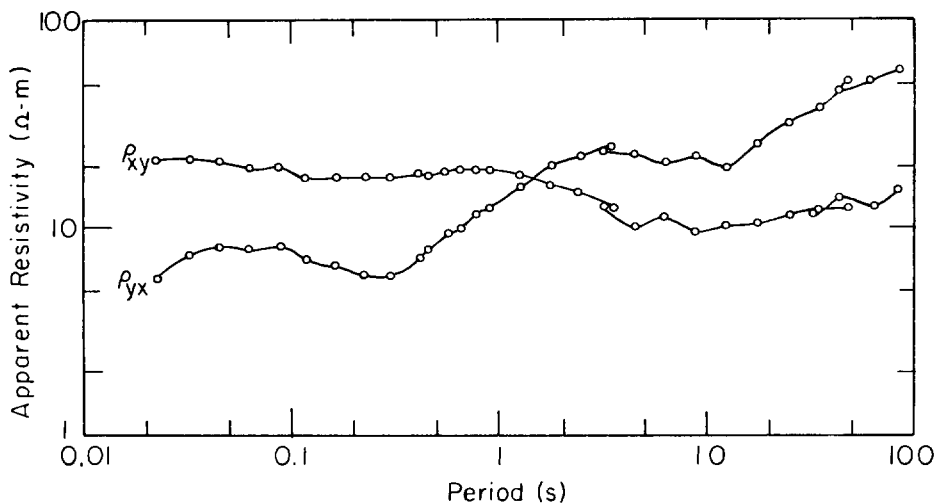


FIG. 13. Remote reference method apparent resistivities versus period, Lower La Gloria.

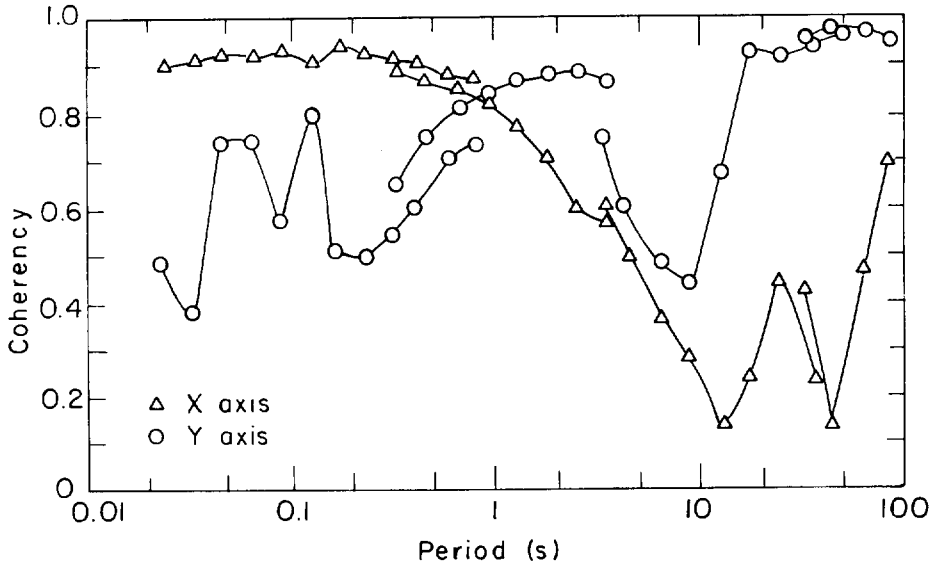


FIG. 14. Coherency between the measured electric field and the electric field predicted by the standard method of analysis, Lower La Gloria.

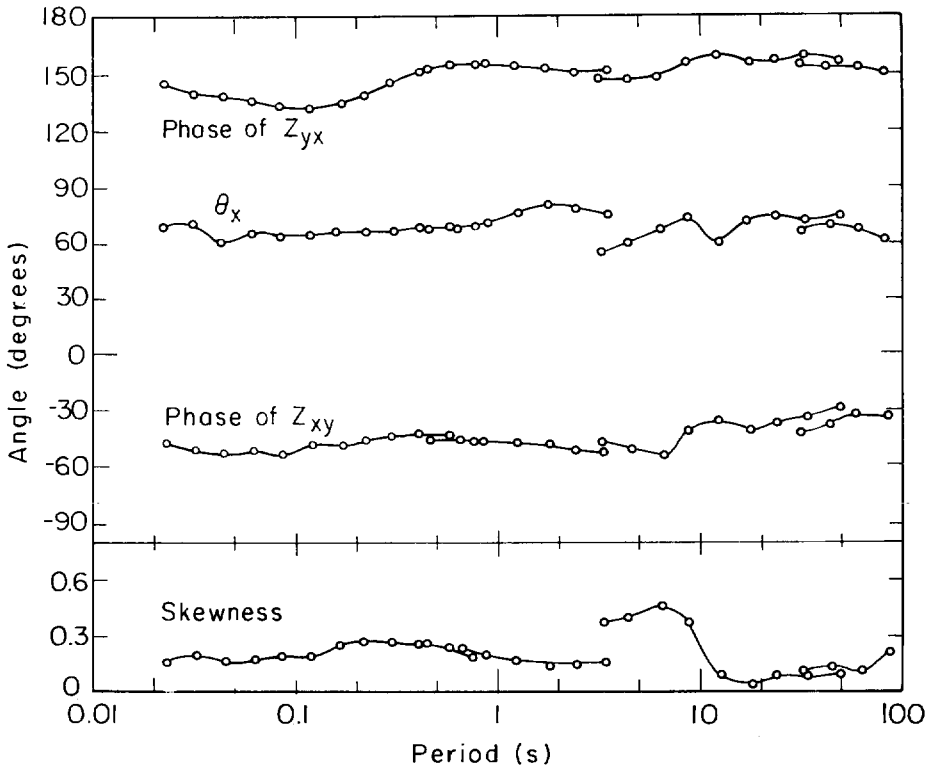


FIG. 15. Orientation angle θ_x between rotated x -axis and magnetic north, skewness, and phase angles versus period, standard method, Lower La Gloria.

QUANTITATIVE EVALUATION OF APPARENT RESISTIVITIES OBTAINED USING REMOTE REFERENCE

In this section we present a more quantitative analysis of the expected errors associated with the apparent resistivities obtained using the remote reference technique. An average disagreement is computed for the apparent resistivities at periods where bands overlap, and a measure of the rms random fluctuations is obtained for the resistivities within a single band.

At both Upper and Lower La Gloria there are three values of ρ_{xy} and three values of ρ_{yx} in band 1 at periods that are also contained in band 2. These resistivities are compared with the linear interpolation of the values of apparent resistivity in band 2. The fractional discrepancy between the overlapping resistivities is computed, and the magnitude of this discrepancy is averaged over each of the three periods, for both axes and for both stations, to produce the "mean discrepancy" for the 12 resistivities in the region of band overlap. In the same way, the mean discrepancy is calculated between the overlaps of bands 2 and 3,

and bands 3 and 4. The mean discrepancies (percent disagreements) and the number of resistivity values compared to obtain each mean discrepancy are shown in Table 3 for both the standard and remote reference analyses.

The mean discrepancies for the remote reference method are consistently smaller than those for the standard analysis. The smallest discrepancy is 1.8 percent between bands 1 and 2. This discrepancy is somewhat smaller than the ± 2 percent uncertainty in apparent resistivity that we expect because of a ± 1 percent uncertainty in amplifier gains. Between bands 2 and 3 and bands 3 and 4, the mean discrepancies are larger, but they are still on the order of the random scatter seen within a single band by comparing apparent resistivities at adjacent periods. Because of the good agreement where the bands overlap, errors due to spectral resolution of the Fourier transform are believed to be negligible. As shown in Table 1, in band 2 the segments are 10 times longer than those in band 1. Thus, the spectral resolution of the harmonics in band 2 is ten times higher than the resolution in

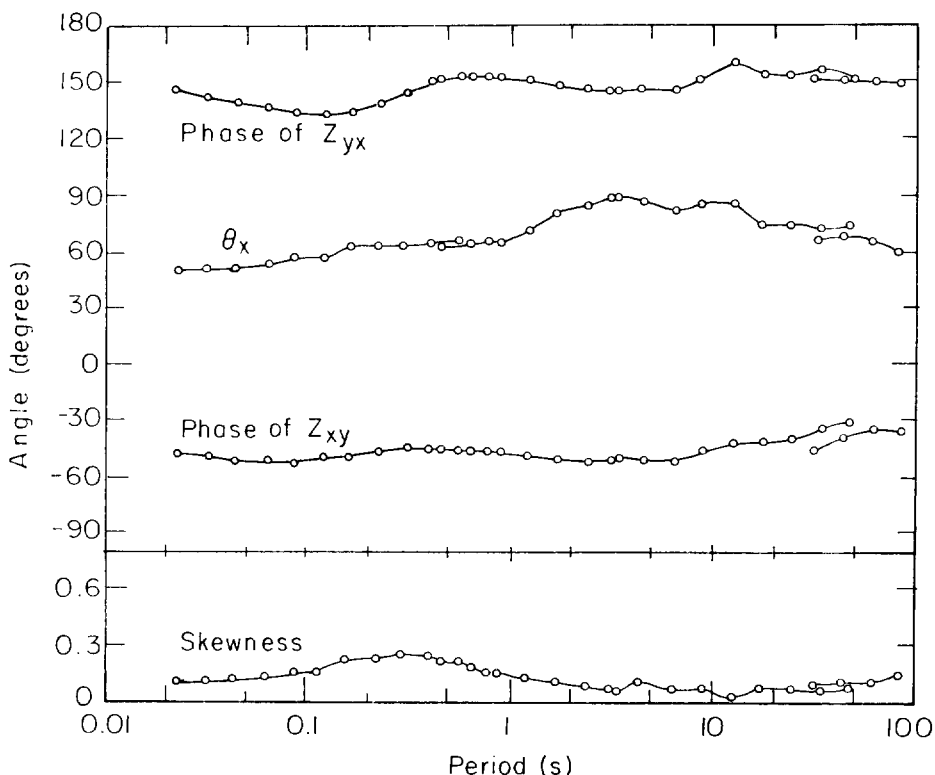


FIG. 16. Orientation angle θ_x between rotated x -axis and magnetic north, skewness, and phase angles versus period, remote reference method, Lower La Gloria.

Table 4. Arrangement of data from bands 1 and 2 into blocks to estimate the standard deviation of the apparent resistivity at each period. Date refers to September 1977.

Band 1				Band 2			
Recording time PST	Date	Data blocks		Recording time	Date	Data blocks	
		Upper La Gloria	Lower La Gloria			Upper La Gloria	Lower La Gloria
11:55 AM–12:00 PM	14	2	Omitted	9:25 AM– 9:50 AM	14	1	1
12:01 PM–12:06 PM	14	3	Omitted	9:55 AM–10:42 AM	14	2	2
7:30 PM– 7:35 PM	14	4	3	10:43 AM–11:27 AM	14	3	3
7:36 PM– 7:41 PM	14	5	4	6:20 PM– 6:57 PM	14	4	4
1:20 PM– 1:25 PM	15	1	1	7:00 PM– 7:32 PM	14	2	2
1:25 PM– 1:30 PM	15	2	2	10:50 AM–11:37 AM	15	1	1
1:30 PM– 1:35 PM	15	3	3	11:38 AM–12:25 PM	15	3	3
1:35 PM– 1:40 PM	15	4	4	12:36 PM– 1:13 PM	15	4	4
1:40 PM– 1:45 PM	15	5	1				
1:45 PM– 1:50 PM	15	1	2				

band 1, and the spectral overlap from narrow peaks in the autopower spectra of the various fields is ten times smaller.

The rms errors associated with apparent resistivities within a single band are now estimated. In Figures 6 and 13 (remote reference analysis), there is no visible scatter between resistivities at adjacent periods for periods shorter than 3 sec (i.e., bands 1 and 2). To estimate the random errors in this range, we recomputed apparent resistivities for each period, using a smaller number of data segments in the determination of the average crosspower densities. The original data segments were sorted into N smaller blocks, thereby obtaining N completely independent estimates for the apparent resistivity at each period. We computed the average of the N values, $\bar{\rho}_j(j = xy, yx)$, and the expected deviation of the mean, defined by (Bendat and Piersol, 1971)

$$\sigma_j = \left[\sum_{i=0}^N (\rho_{ij} - \bar{\rho}_j)^2 / N(N-1) \right]^{1/2}. \quad (10)$$

For band 1 at Upper La Gloria $N = 5$ blocks were used, while for band 1 at Lower La Gloria and for band 2 at both stations $N = 4$ blocks were used. In an attempt to include signals of various polarizations in each of the N blocks of data segments, roughly equal numbers of records were selected for each block from two different recording times that were widely separated. Table 4 summarizes the recording times and the number of the block to which the data segments were assigned. There are no entries for the first two recording times in band 1 at Lower La Gloria because we had accidentally removed a set of preamplifiers from some of the channels at that station.

Table 5 lists the percentage expected deviation of the mean resistivity, $100 \sigma_j / \bar{\rho}_j$, as a function of period for both stations. We see that the expected

fractional deviation of both $\bar{\rho}_{xy}$ and $\bar{\rho}_{yx}$ is always less than 5 percent and, for 87 percent of the data, is 2 percent or less. The average of $\sigma_j / \bar{\rho}_j$ over all entries in Table 5 is 1.3 percent. For comparison, when we performed the same analysis on the apparent resistivities calculated by the standard analysis, the average of the fractional standard deviation was 3.3 percent. At periods less than 3 sec, the expected deviations are much smaller than the discrepancies caused by bias (typically 20 percent) that one observes when comparing these results with those obtained using the remote reference analysis.

ORIENTATION ANGLES, PHASES, AND SKEWNESSES

Graphs of the other parameters that may be used in modeling the resistivity of the earth are now examined. For Upper La Gloria, Figures 8 and 9 show the orientation angles θ_x between the rotated x -axes and magnetic north, the phases of Z_{xy} and Z_{yx} , and the skewness as a function of period for the standard and remote reference analyses. A right-handed coordinate system is used with the z -axis pointing down, and the complex phase is $-i\omega t$. The corresponding results for Lower La Gloria are shown in Figures 15 and 16. From Figures 8 and 9 we see that at Upper La Gloria both methods of analysis give physically reasonable values for the orientation angle, phases, and skewness. There is a maximum scatter of about ± 10 degrees in the phases and ± 5 degrees in the orientation angle for both methods at periods near 10 sec. For both methods, the phase angles where bands 3 and 4 overlap differ by about 5 degrees. However, at periods shorter than 0.1 sec the standard analysis yields a scatter of about ± 3 degrees in orientation angle whereas the remote reference yields no visible scatter. At Lower La Gloria the standard and remote

reference methods yield very similar values for the phase angles, with scatter increasing with period up to about ± 5 degrees for periods longer than 10 sec (Figures 15 and 16). The standard analysis yields values of orientation angle and skewness that differ by 20 degrees and 0.2 respectively between bands 2 and 3, while no disagreements are apparent for the remote reference method. There are also consistent differences between the two methods. For example, the orientation angle at short periods determined by the remote reference method is about 52 degrees, while by the standard method it is about 65 degrees.

SUMMARY AND DISCUSSION

The technical feasibility of performing MT soundings using a remote magnetometer as a reference has been demonstrated, and the results from this method are shown to be substantially better than those obtained using the conventional MT technique. Smooth curves of apparent resistivities, orientation angles, phases, and skewnesses as functions of period for both stations were obtained, even at periods where the coherencies determined from the standard analysis were as low as 0.1. In bands 1 and 2 (periods < 3 sec) an estimate of 1.3 percent was obtained for the mean percentage error associated with random variations in the apparent resistivities. At periods where bands 1 and 2 overlapped, the resistivities obtained for the two bands agreed to within an average percentage uncertainty of 1.8 percent.

By comparing apparent resistivities from the re-

mote reference analysis with apparent resistivities from the standard impedance and admittance analyses, we demonstrated the significance of the bias errors in these least squares methods, and showed that, in general, there is bias from noise in both electric and magnetic channels. In bands 1 and 2, where the coherency was between 0.7 and 0.9, the dominant bias was from noise in the magnetic channels, and was typically of the order of 20 percent. At Lower La Gloria, where the coherencies were as low as 0.1, the standard analysis apparent resistivities at periods near 10 sec were biased downward by more than two orders of magnitude, while the apparent resistivities from the admittance method were biased upward by one order of magnitude. The apparent resistivities for the crosspower analysis (which is unbiased by autopower noise) had random errors that often exceeded the bias errors of the two least-squares methods.

The results for the remote reference analysis are unbiased by noise in autopowers and by noises that are not correlated over the distance separating the reference magnetometer and the base station. The possibility of systematic errors caused by long range correlations in the noises cannot be ruled out entirely, but it is believed that the use of the remote reference greatly reduces the likelihood of such systematic errors.

As an alternative to a remote magnetic reference, one could consider using a remote telluric array. However, there are two reasons why telluric arrays may

Table 5. Expected standard deviations, $100 \sigma_j / \bar{\rho}_j$, of mean apparent resistivities from the remote reference method.

Period (sec)	Upper La Gloria		Lower La Gloria	
	$100 \sigma_{xy} / \bar{\rho}_{xy}$	$100 \sigma_{yx} / \bar{\rho}_{yx}$	$100 \sigma_{xy} / \bar{\rho}_{xy}$	$100 \sigma_{yx} / \bar{\rho}_{yx}$
0.03	0.4	3.5	2.0	2.3
0.04	0.5	0.8	0.7	0.8
0.06	0.2	0.8	1.3	0.5
0.08	0.3	2.1	1.1	0.9
0.12	0.5	0.7	0.8	0.7
0.16	0.4	1.4	1.6	1.3
0.22	0.7	0.6	1.9	1.1
0.30	0.6	0.9	0.9	1.8
0.41	0.04	4.4	0.7	1.2
0.57	1.2	2.2	1.3	1.3
0.79	1.2	1.6	1.8	1.5
0.33	2.2	1.6	0.4	0.8
0.45	0.8	1.0	1.2	0.5
0.63	1.2	3.0	1.0	0.5
0.88	1.2	0.9	0.9	0.7
1.2	1.0	1.3	1.4	1.1
1.7	1.1	1.4	0.9	1.5
2.4	0.8	3.4	2.7	1.2
3.4	1.3	2.6	1.7	2.0

prove to be less reliable as a reference than a magnetic field reference. First, it has been our experience that there is often more noise in the electric measurements than in the magnetic, although this was not the case at the La Gloria stations. Second, the electric field at the surface of the earth produced by a given magnetic field is highly dependent on the geology. The reference must be able to respond in different directions as the polarization of the incident magnetic field changes. If the apparent resistivity is highly anisotropic, the electric field response tends to lie in the direction of the highest apparent resistivity, and a higher level of random error is produced by a given level of random noise.

The use of a remote magnetic reference should enable one to carry out a magnetotelluric survey in an area contaminated by cultural magnetic and electric noises, provided that the reference is sufficiently distant to insure that any possible bias errors due to correlated noises are small compared with the random errors. Clearly, the minimum separation depends on both the correlation lengths of the noises and on the length of time over which the data are averaged. The upper limit on the separation is set not only by practical problems of telemetry but also by the coherence length of incoming magnetic signals. When the separation becomes greater than the coherence length, the random errors will increase.

The use of a remote reference may enable one to test the validity of the assumptions usually made in magnetotellurics: for example, that the incident fields are plane waves, and that the electric fields are adequately determined by measurements of the potential difference between widely separated electrodes. The plane wave approximation could be tested by measuring the apparent resistivities as a function of time in an auroral zone (where source effects are likely to be largest) over ground where the true resistivity is believed to be constant. One could examine the effects of electrode placement on the apparent resistivity by measuring apparent resistivities as a function of electrode position. Furthermore, the remote reference technique should allow one to monitor long term changes in the apparent resistivity at a given site to greater accuracy than has previously been possible.

Finally, the additional cost of the second magneto-

telluric station is believed to be easily justified economically, in view of the advantages of the remote reference technique. First, apart from data rejected in a preliminary screening, all of the data collected were used to make reliable estimates of the apparent resistivities, even when the coherencies computed by the standard method were as low as 0.1. Second, the simultaneous operation of the magnetotelluric stations obviously doubles the surveying rate compared with a single station. Thus, the remote reference technique may substantially reduce the time necessary to survey a given area.

ACKNOWLEDGMENTS

We are grateful to Mr. Melendy and Mr. DeRosa for granting us access to their land. We are indebted to Professor H. F. Morrison and his students for the loan of equipment and for invaluable assistance. Professor Morrison and Dr. K. Vozoff kindly made helpful comments on the manuscript. This work was supported by the Divisions of Basic Energy Sciences and of Geothermal Energy, U.S. Department of Energy, and by the U.S.G.S. under grant number 14-08-0001-G-328.

REFERENCES

- Bendat, J. S., and Piersol, A. G., 1971, *Random data: Analysis and measurement procedures*: New York, John Wiley and Sons, Inc.
- Clarke, J., Goubau, W. M., and Ketchen, M. B., 1976, Tunnel junction dc SQUID: fabrication, operation, and performance: *J. Low Temp. Phys.*, v. 25, p. 99-144.
- Goubau, W. M., Gamble, T. D., and Clarke, J., 1978, Magnetotelluric data analysis: removal of bias: *Geophysics*, v. 43, p. 1157-1169.
- Kao, D. W., and Rankin, D., 1977, Enhancement of signal to noise ratio in magnetotelluric data: *Geophysics*, v. 42, p. 103-110.
- Mazella, A. T., 1976, *Deep resistivity study across the San Andreas fault zone*: Ph.D. thesis, University of California, Berkeley (137 pages).
- Morrison, H. F., Corwin, R. F., and Chang, M., 1977, High accuracy determination of temporal variations of crustal resistivity: *in* The nature and physical properties of the earth's crust, J. G. Heacock, Ed., AGU Monograph 20: p. 593-618.
- Sims, W. E., Bostick, F. X., Jr., and Smith, H. W., 1971, The estimation of magnetotelluric impedance tensor elements from measured data: *Geophysics*, v. 36, p. 938-942.
- Vozoff, K., 1972, The magnetotelluric method in the exploration of sedimentary basins: *Geophysics*, v. 37, p. 98-141.